

A closure method for random advection of a passive scalar

James P. Gleeson*

Applied Mathematics, Caltech, Pasadena, CA 91125

Email: gleeson@math.la.asu.edu,

telephone: (480) 965 2352,

fax: (480) 965 0461.

Revised January 27, 2000.

Abstract

A novel functional method is applied to calculate the statistics of a passive scalar in an isotropic turbulent velocity field. The method yields asymptotic series expansions for small velocity correlation time, from which approximate closure equations are derived. The closure method admits a diagram expansion, and is implemented as a *Mathematica* program. Padé summation of the asymptotic series yields accurate values for the effective diffusivity and gives formulas expressing the Lagrangian correlation of the velocity in terms of the Eulerian correlation. The approximations compare very favorably with numerical simulations of advection by a Gaussian velocity field.

*Current address: Department of Mathematics, Arizona State University, Tempe AZ 85287-1804.

1 Introduction

When a pollutant tracer or small amount of heat is transported (or *advected*) by a turbulent fluid, it does not significantly affect the flow by its presence. Such a quantity is therefore called a *passive scalar*. Since the advecting fluid is in turbulent motion, it can only be described by its statistical characteristics, notably the mean value of the fluid velocity and the energy spectrum of the flow. It is to be expected that the passive scalar will also require such a statistical representation. An outstanding problem in fluid mechanics is to describe the statistics of the scalar, given the velocity statistics.

In particular, there is considerable interest¹⁻³ in the calculation of the mean scalar concentration, the dispersion rate of tracers and the effective (or “turbulent”) diffusivity. The effective diffusivity has been examined by various workers using different closure schemes, e.g., Roberts’⁴ application of Kraichnan’s⁵ direct interaction approximation and the self-consistent theory of Phythian and Curtis.³ In this work, we introduce a functional method which enables us to derive successively improving closure approximations. We generate a diagram expansion similar to that employed by Dean et al.² for time-independent Gaussian velocity fields, and demonstrate the interpretation of the diagram series as an asymptotic series in the velocity correlation time, denoted by τ_* . Thus, τ_* is the characteristic time over which the velocity remains appreciably correlated. The vanishing τ_* limit leads to a white-noise (delta-correlated) advecting velocity, which was introduced by Kraichnan⁶ and has attracted considerable recent attention, particularly in regard to the anomalous scaling of the scalar moments.⁷⁻¹⁰ Silant’ev¹¹ notes the possibility of using an iteration scheme to generate an expansion in τ_* for the long-term effective diffusivity, but highlights its poor convergence in the physically relevant case $\tau_* u/l = O(1)$, i.e., when the velocity correlation time is on the order of the eddy circulation time. (Here l is the integral scale of the turbulent velocity field and u is its r.m.s. value). The importance of this case is highlighted by the available data on the velocity correlation function in turbulent flows—see, for example, the experimental results of Comte-Bellot and Corrsin¹² and

the numerical calculations of Sanada and Shanmugasundaram¹³ and McComb et al.¹⁴ We implement the diagram rules as an algorithm, using the symbolic manipulation capabilities of *Mathematica*, and calculate up to five terms in the τ_* power series for the long-term effective diffusivity. Silant'ev argues that such a series is useful only for very short correlation times, but we show the corresponding Padé approximations converge rapidly and give accurate results, even when τ_* is on the order of the eddy circulation time.

Predictions of tracer dispersion and pollutant spread are most easily expressed in terms of the Lagrangian velocity correlation, i.e., the correlation measured when following a fluid particle (see Taylor,¹⁵ Csanady¹). On the other hand, experimental data is almost always measured at fixed points, giving the so-called Eulerian correlation functions (or spectra). A classical turbulence problem is the determination of a connection between the Lagrangian and Eulerian correlation functions—see, for example, Saffman's¹⁶ application of Corrsin's conjecture¹⁷ to obtain a quasi-normal type closure. This and related methods are reviewed in the context of one-dimensional fields by Davis.¹⁸ A simple generalization of the method outlined above allows us to write Padé-type approximations which give explicit expressions for the Lagrangian velocity correlation in terms of the Eulerian correlation functions. We perform numerical simulations of Gaussian velocity fields and find the approximations for the effective diffusivity and the Lagrangian correlation to be accurate for correlation times which are on the order of the eddy circulation time.

Consider the advection of a passive scalar $\theta(\mathbf{x}, t)$ (representing, say, pollutant concentration) by a random, three-dimensional, incompressible velocity field $\mathbf{u}(\mathbf{x}, t)$:

$$\frac{\partial}{\partial t}\theta + \mathbf{u} \cdot \nabla\theta - \kappa_0\nabla^2\theta = 0 \tag{1}$$

where κ_0 is the molecular diffusivity. The velocity can be calculated by solving the Navier-Stokes equations (at least in principle, if not often in practice), but for simplicity here we will suppose it to be a Gaussian (i.e., multivariate normal) random function with known correlation $\langle u_\alpha(\mathbf{x}, t)u_\beta(\mathbf{x}', t') \rangle$. We will further assume the velocity statistics to be homogeneous and isotropic.

If we take the initial condition for the passive scalar equation (1) to be

$$\theta(\mathbf{x}, 0) = \delta(\mathbf{x}), \quad (2)$$

then $\theta d\mathbf{x}$ is the probability, for one realization (i.e., an experiment giving $\mathbf{u}(\mathbf{x}, t)$) of the turbulence, that a marked particle which was at the origin at time $t = 0$ will be in the volume element $d\mathbf{x}$ at time t . The average probability density $\langle \theta(\mathbf{x}, t) \rangle$ is found by averaging over the velocity statistics. The *dispersion* or *mean-square displacement* of the marked particles at a time t is a measurement of their distance from the source at the origin and can be calculated as

$$D(t) = \frac{1}{3} \int x_\alpha x_\alpha \langle \theta(\mathbf{x}, t) \rangle d\mathbf{x}, \quad (3)$$

with summation over repeated indices and integration over all of space. The quantity

$$\kappa(t) = \frac{1}{2} \frac{dD(t)}{dt} \quad (4)$$

is often called the *effective diffusivity* or *eddy diffusivity*. These names arise from the use of this quantity in diffusion equation approximations for turbulent advection.¹

Averaging equations (1) and (2) yields the following equations for the mean concentration $\Theta(\mathbf{x}, t) = \langle \theta(\mathbf{x}, t) \rangle$:

$$\frac{\partial}{\partial t} \Theta - \kappa_0 \nabla^2 \Theta = -\nabla \cdot \langle \mathbf{u} \theta \rangle.$$

Evaluation of the term $\langle \mathbf{u} \theta \rangle$ is complicated by the fact that θ is a non-trivial functional of the random velocity \mathbf{u} . In the next section we outline a method for expanding $\langle \mathbf{u} \theta \rangle$ as an infinite series which may be truncated to give integrodifferential approximating equations for $\Theta(\mathbf{x}, t)$. Having obtained equations for Θ in this manner, we may calculate series approximations to the dispersion $D(t)$ and the effective diffusivity $\kappa(t)$ according to equations (3) and (4).

2 The Functional Derivative Closure

Exposition of our method is eased by transforming the governing equations to wavenumber space, i.e., writing them in terms of Fourier-transformed variables such as

$$\theta(\mathbf{k}, t) = \frac{1}{(2\pi)^3} \int \theta(\mathbf{x}, t) e^{-i\mathbf{k}\cdot\mathbf{x}} d\mathbf{x}.$$

(Henceforth we consider only such Fourier-transformed variables and so can use the same symbol as in physical space without ambiguity). The transform of equations (1) and (2) yields the following pair of equations for $\theta(\mathbf{k}, t)$:

$$\frac{\partial}{\partial t} \theta + \kappa_0 k^2 \theta = -i \int (\mathbf{k} - \mathbf{p}) \cdot \mathbf{u}(\mathbf{p}, t) \theta(\mathbf{k} - \mathbf{p}, t) d\mathbf{p} \quad (5)$$

$$\theta(\mathbf{k}, 0) = 1, \quad (6)$$

which may be averaged as above to find equations for $\Theta(\mathbf{k}, t) = \langle \theta(\mathbf{k}, t) \rangle$:

$$\begin{aligned} \frac{\partial}{\partial t} \Theta + \kappa_0 k^2 \Theta &= -i \int (\mathbf{k} - \mathbf{p}) \cdot \langle \mathbf{u}(\mathbf{p}, t) \theta(\mathbf{k} - \mathbf{p}, t) \rangle d\mathbf{p} \\ \Theta(\mathbf{k}, 0) &= 1. \end{aligned} \quad (7)$$

Again the difficulty is the evaluation of the stochastically nonlinear term $\langle \mathbf{u}\theta \rangle$.

We introduce the *functional derivative closure* method (FDC hereafter, for further details see Ref. 19). The goal is the representation of $\langle \mathbf{u}\theta \rangle$ as an infinite series, truncations of which give closed equations for Θ . The FDC series is generated by repeated application of a theorem due to E. A. Novikov:²⁰

Theorem 1 (Novikov, 1965) *For Gaussian random functions $u_\alpha(\mathbf{p}, t)$ with zero mean, the cross-correlation $\langle u_\alpha(\mathbf{p}, t) F[\mathbf{u}] \rangle$ may be computed as*

$$\langle u_\alpha(\mathbf{p}, t) F[\mathbf{u}] \rangle = \int_0^\infty dt_1 \int d\mathbf{p} \langle u_\alpha(\mathbf{p}, t) u_\beta(\mathbf{q}, t_1) \rangle \left\langle \frac{\delta F[\mathbf{u}]}{\delta u_\beta(\mathbf{q}, t_1)} \right\rangle.$$

Here F stands for any functional of \mathbf{u} .

In particular, taking $F[\mathbf{u}] = \theta(\mathbf{k} - \mathbf{p}, t)$, we have

$$\langle u_\alpha(\mathbf{p}, t)\theta(\mathbf{k} - \mathbf{p}, t) \rangle = \int_0^\infty dt_1 Q_{\alpha\beta}(\mathbf{p}, t - t_1) \left\langle \frac{\delta\theta(\mathbf{k} - \mathbf{p}, t)}{\delta u_\beta(-\mathbf{p}, t_1)} \right\rangle, \quad (8)$$

where $Q_{\alpha\beta}$ is defined by the relation for homogeneous stationary turbulence:

$$\langle u_\alpha(\mathbf{k}, t)u_\beta(\mathbf{p}, t_1) \rangle = \delta(\mathbf{k} + \mathbf{p})Q_{\alpha\beta}(\mathbf{k}, t - t_1).$$

For incompressible velocity with isotropic and stationary statistics, $Q_{\alpha\beta}$ may be written²¹

$$Q_{\alpha\beta}(\mathbf{k}, \tau) = \frac{E(k)R(\tau, k)}{4\pi k^2} \left(\delta_{\alpha\beta} - \frac{k_\alpha k_\beta}{k^2} \right),$$

where $E(k)$ is the usual energy spectrum and $R(\tau, k)$ is the time correlation function of the velocity (with $R(0, k) = 1$).

An aside on functional differentiation is in order here. The standard definition (e.g., Ref. 22) obeys the rules of normal differentiation, i.e.,

$$\begin{aligned} \frac{\delta}{\delta f(x)} \{F_1[f] + F_2[f]\} &= \frac{\delta F_1[f]}{\delta f(x)} + \frac{\delta F_2[f]}{\delta f(x)} \\ \frac{\delta}{\delta f(x)} \{F_1[f]F_2[f]\} &= F_1[f] \frac{\delta F_2[f]}{\delta f(x)} + \frac{\delta F_1[f]}{\delta f(x)} F_2[f], \end{aligned}$$

and

$$\frac{\delta f(y)}{\delta f(x)} = \delta(x - y).$$

In order to apply Novikov's theorem (8), a formal solution of (5) for $\theta(\mathbf{k} - \mathbf{p}, t)$ is written as:

$$\theta(\mathbf{k} - \mathbf{p}, t) = e^{-\kappa_0|\mathbf{k}-\mathbf{p}|^2 t} - i \int_0^t dt_2 e^{-\kappa_0|\mathbf{k}-\mathbf{p}|^2(t-t_2)} \int d\mathbf{q} (\mathbf{k} - \mathbf{p} - \mathbf{q}) \cdot \mathbf{u}(\mathbf{q}, t_2)\theta(\mathbf{k} - \mathbf{p} - \mathbf{q}, t_2). \quad (9)$$

This is simply the integral equation corresponding to the differential equation (5) with initial condition (6). Taking the functional derivative and averaging yields

$$\begin{aligned} \left\langle \frac{\delta\theta(\mathbf{k} - \mathbf{p}, t)}{\delta u_\beta(-\mathbf{p}, t_1)} \right\rangle &= -ie^{-\kappa_0|\mathbf{k}-\mathbf{p}|^2(t-t_1)} k_\beta \langle \theta(\mathbf{k}, t_1) \rangle \\ &\quad - i \int_0^t dt_2 e^{-\kappa_0|\mathbf{k}-\mathbf{p}|^2(t-t_2)} \int d\mathbf{q} (\mathbf{k} - \mathbf{p} - \mathbf{q}) \cdot \left\langle \mathbf{u}(\mathbf{q}, t_2) \frac{\delta\theta(\mathbf{k} - \mathbf{p} - \mathbf{q}, t_2)}{\delta u_\beta(-\mathbf{p}, t_1)} \right\rangle. \end{aligned} \quad (10)$$

The second term on the right-hand side contains an integrand of form $\langle u_\alpha F[\mathbf{u}] \rangle$, and so it may be expanded by applying Novikov's theorem again. If, instead, we ignore the second term and consider the first term on the right-hand side of (10) as a first approximation to $\langle \delta\theta/\delta u_\beta \rangle$, then Novikov's theorem (8) gives a first approximation to (7):

$$\frac{\partial}{\partial t}\Theta + \kappa_0 k^2 \Theta = - \int_0^t dt_1 \int d\mathbf{p} (k_\alpha - p_\alpha) Q_{\alpha\beta}(\mathbf{p}, t - t_1) k_\beta e^{-\kappa_0 |\mathbf{k} - \mathbf{p}|^2 (t - t_1)} \Theta(\mathbf{k}, t_1), \quad (11)$$

and we call this the *FDC1 approximation* to (7). Note this is a closed equation for Θ , the solution of which gives an approximation to the exact average probability density. The correction to this approximation is found by applying Novikov's theorem to the second term on the right-hand side of (10). This correction involves a second order functional derivative, which is evaluated from the formal solution (9) and another application of Novikov's theorem. Successive applications of Novikov's theorem to higher functional derivatives of (9) enable us to approximate the right-hand side of (7) as a series of integrals over Θ , each weighted by multiple factors of $Q_{\alpha\beta}$. The *FDCn approximation* is defined to be the truncation of this series which contains the integrals over m factors of $Q_{\alpha\beta}$, for all $m \leq n$. Thus, the FDC2 approximation to (7) contains

integrals in which \mathbf{Q} appears once and twice:

$$\begin{aligned}
\frac{\partial}{\partial t}\Theta(\mathbf{k}, t) + \kappa_0 k^2 \Theta(\mathbf{k}, t) = & \\
& - \int_0^t dt_1 \int d\mathbf{p} [(\mathbf{k} - \mathbf{p}) \cdot \mathbf{Q}(\mathbf{p}, t - t_1) \cdot \mathbf{k}] e^{-\kappa_0 |\mathbf{k} - \mathbf{p}|^2 (t - t_1)} \Theta(\mathbf{k}, t_1) \\
& + \int_0^t dt_2 \int_0^{t_2} dt_1 \int_0^{t_1} dt_3 \iint d\mathbf{p} d\mathbf{q} \left\{ [(\mathbf{k} - \mathbf{p}) \cdot \mathbf{Q}(\mathbf{p}, t - t_1) \cdot (\mathbf{k} - \mathbf{q})] \right. \\
& \quad \times [(\mathbf{k} - \mathbf{p} - \mathbf{q}) \cdot \mathbf{Q}(\mathbf{q}, t_2 - t_3) \cdot \mathbf{k}] \\
& \quad \left. \times e^{-\kappa_0 [|\mathbf{k} - \mathbf{p}|^2 (t - t_2) + |\mathbf{k} - \mathbf{p} - \mathbf{q}|^2 (t_2 - t_1) + |\mathbf{k} - \mathbf{q}|^2 (t_1 - t_3)]} \right\} \Theta(\mathbf{k}, t_3) \\
& + \int_0^t dt_2 \int_0^{t_2} dt_3 \int_0^{t_3} dt_1 \iint d\mathbf{p} d\mathbf{q} \left\{ [(\mathbf{k} - \mathbf{p}) \cdot \mathbf{Q}(\mathbf{p}, t - t_1) \cdot \mathbf{k}] \right. \\
& \quad \times [(\mathbf{k} - \mathbf{p} - \mathbf{q}) \cdot \mathbf{Q}(\mathbf{q}, t_2 - t_3) \cdot (\mathbf{k} - \mathbf{p})] \\
& \quad \left. \times e^{-\kappa_0 [|\mathbf{k} - \mathbf{p}|^2 (t - t_2) + |\mathbf{k} - \mathbf{p} - \mathbf{q}|^2 (t_2 - t_3) + |\mathbf{k} - \mathbf{p}|^2 (t_3 - t_1)]} \right\} \Theta(\mathbf{k}, t_1).
\end{aligned} \tag{12}$$

We have adopted the notation $\mathbf{k} \cdot \mathbf{Q} \cdot \mathbf{p} \equiv k_\alpha Q_{\alpha\beta} p_\beta$.

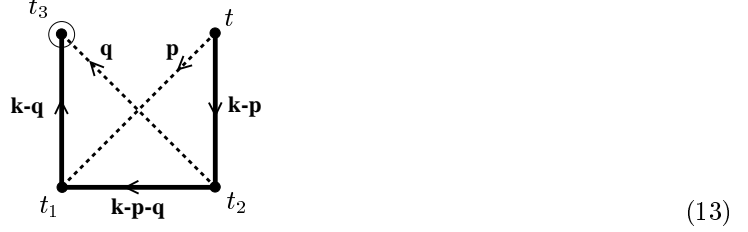
In the next section we introduce the diagram expansion, which allows us to concisely represent the complicated approximation equations like (12) in terms of geometrical diagrams. This representation also facilitates the implementation of the approximation scheme in *Mathematica* (see section 5).

3 Diagram expansions

Clearly the FDC approximation equations quickly become very complicated to write down. However, the equations may be reproduced from a diagram expansion by applying a few simple diagram rules. Diagram expansions are an accepted bookkeeping device for perturbation series.^{2,23,24} First, define the *diagrams of order n* to be n -polygons with dotted lines joining pairs of vertices. Then the *FDC diagrams of order n* are those diagrams of order n which are *connected*, i.e., which cannot be split into two separate parts by cutting one solid line. For example, the FDC diagrams of order 1 and 2 (which represent the FDC2

approximation (12) above) are shown in Fig. 1. The FDC equation is recovered from the diagrams by applying the following diagram rules.

Consider the diagram



which represents the first FDC2 term

$$\int_0^\infty dt_2 \int_0^\infty dt_1 \int_0^\infty dt_3 H_{tt_2} H_{t_2 t_1} H_{t_1 t_3} \iint d\mathbf{p} d\mathbf{q} [(\mathbf{k} - \mathbf{p}) \cdot \mathbf{Q}(\mathbf{p}, t - t_1) \cdot (\mathbf{k} - \mathbf{q})] \\ \times [(\mathbf{k} - \mathbf{p} - \mathbf{q}) \cdot \mathbf{Q}(\mathbf{q}, t_2 - t_3) \cdot \mathbf{k}] e^{-\kappa_0 [|\mathbf{k} - \mathbf{p}|^2(t - t_2) + |\mathbf{k} - \mathbf{p} - \mathbf{q}|^2(t_2 - t_1) + |\mathbf{k} - \mathbf{q}|^2(t_1 - t_3)]} \Theta(\mathbf{k}, t_3). \quad (14)$$

Here H_{ts} represents the Heaviside function

$$H_{ts} = \begin{cases} 1 & \text{if } t > s, \\ 0 & \text{otherwise} \end{cases}$$

Observe that (14) may be produced from (13) by applying the following rules:

1. Vertex labels are the time integration variables, except for the first vertex (which is always labeled t).
2. The time integral limits are determined by associating a factor of $H_{t_i t_j}$ with the solid line joining vertices labeled t_i and t_j .
3. The wavevector integration variables are the wavevectors labeling the internal dotted lines; these integrals are over all wavevector space.

4. The vector sum of wavevectors at each vertex is zero, except for the first vertex (labeled t) which has sum $+\mathbf{k}$, and the final (circled) vertex which has sum $-\mathbf{k}$.

To compose the integrand, we multiply the factors resulting from each of the following rules:

5. For each internal dotted line, consider the start and end vertices. For example, in (13) for the internal dotted line labeled \mathbf{p} , the start vertex is labeled t and the end vertex is labeled t_1 . Both the start and the end vertex have solid lines emanating from them; suppose the wavevector labels on these lines are \mathbf{a} and \mathbf{b} respectively. Then the factor we seek is $-\mathbf{a} \cdot \mathbf{Q}(\mathbf{p}, t - t_1) \cdot \mathbf{b}$ where \mathbf{p} is the dotted line label and t and t_1 are the start and end vertex labels. (If the end vertex is the circled vertex, then let $\mathbf{b} = \mathbf{k}$). In the example (13), $\mathbf{a} = \mathbf{k} - \mathbf{p}$ and $\mathbf{b} = \mathbf{k} - \mathbf{q}$, so that the factor is $-(\mathbf{k} - \mathbf{p}) \cdot \mathbf{Q}(\mathbf{p}, t - t_1) \cdot (\mathbf{k} - \mathbf{q})$. By applying this rule again to the second dotted line, we find another factor of $-(\mathbf{k} - \mathbf{p} - \mathbf{q}) \cdot \mathbf{Q}(\mathbf{q}, t_2 - t_3) \cdot \mathbf{k}$.
6. For each solid line joining t_i to t_j say, and labeled by \mathbf{a} , multiply by a factor of $\exp(-\kappa_0 |\mathbf{a}|^2 (t_i - t_j))$. In the example (13) this gives us three factors of $\exp(-\kappa_0 |\mathbf{k} - \mathbf{p}|^2 (t - t_2))$, $\exp(-\kappa_0 |\mathbf{k} - \mathbf{p} - \mathbf{q}|^2 (t_2 - t_1))$ and $\exp(-\kappa_0 |\mathbf{k} - \mathbf{q}|^2 (t_1 - t_3))$.
7. Finally, the circled vertex carries a factor of $\Theta(\mathbf{k}, t_i)$, where t_i is the label of the circled vertex.

These rules form an algorithm for finding the FDC equations and so may be implemented using a symbolic manipulation program like *Mathematica*.

Recalling the definition (3) of the dispersion $D(t)$, we find

$$D(t) = -(2\pi)^3 \frac{1}{3} \frac{\partial^2}{\partial k_\alpha \partial k_\alpha} \Theta(\mathbf{k}, t) \Big|_{\mathbf{k}=\mathbf{0}}. \quad (15)$$

This relation allows us to find expressions for the dispersion (or more readily the effective diffusivity $\dot{D}/2$) from the FDC evolution equations for $\Theta(\mathbf{k}, t)$, for example (12). Taking the evolution equation for $\Theta(\mathbf{k}, t)$,

applying the operator $-(2\pi)^3 \frac{1}{3} \frac{\partial^2}{\partial k_\alpha \partial k_\alpha}$, then setting \mathbf{k} to zero (and noting $\Theta(0, t) = (2\pi)^{-3}$ since Θ is a probability density) yields the FDC2 equation for the effective diffusivity $\kappa(t) = \frac{1}{2} \frac{dD}{dt}$:

$$\kappa(t) = \kappa_0 + \kappa_1(t) + \kappa_2(t), \quad (16)$$

with

$$\kappa_1(t) = \frac{2}{3} \int_0^t dt_1 \int \frac{d\mathbf{p}}{4\pi p^2} E(p) R(t-t_1, \mathbf{p}) e^{-\kappa_0 p^2 (t-t_1)},$$

and

$$\begin{aligned} \kappa_2(t) = & -\frac{1}{3} \int_0^t dt_2 \int_0^{t_2} dt_1 \int_0^{t_1} dt_3 \iint \frac{d\mathbf{p} d\mathbf{q}}{(4\pi p q)^2} \left\{ p q \mu (\mu^2 - 1) E(p) E(q) R(t-t_1, \mathbf{p}) R(t_2-t_3, \mathbf{q}) \right. \\ & \times e^{-\kappa_0 [p^2(t-t_2) + (p^2+q^2+2pq\mu)(t_2-t_1) + q^2(t_1-t_3)]} \\ & \left. + 2p^2(1-\mu^2) E(p) E(q) R(t-t_3, \mathbf{p}) R(t_2-t_1, \mathbf{q}) e^{-\kappa_0 [p^2(t-t_2) + (p^2+q^2+2pq\mu)(t_2-t_1) + p^2(t_1-t_3)]} \right\}. \end{aligned}$$

We denote by μ the cosine of the angle between \mathbf{p} and \mathbf{q} , i.e., $\mu = \mathbf{p} \cdot \mathbf{q} / pq$. Here $\kappa_n(t)$ represents the new term appearing in the FDC n approximation and (16) is the truncation at order two of the series

$$\kappa(t) = \kappa_0 + \sum_{n=1}^{\infty} \kappa_n(t). \quad (17)$$

In Ref. 19 it is demonstrated that

$$\kappa_n(t) = O(\tau_*^{2n-1}) \quad \text{as} \quad \tau_* \rightarrow 0,$$

where τ_* denotes the velocity correlation time, nondimensionalized by, say, the eddy circulation time. In other words, the series (17) is an asymptotic series for small velocity correlation time. In section 5 we consider truncations of this series—for example (16)—each of which yields a quadrature expression for the effective diffusivity $\kappa(t)$, depending only on the energy spectrum $E(k)$ and the time correlation function $R(\tau, k)$. The diagram rules for Θ are easily generalized to give a diagram-based algorithm for the FDC series for $\kappa(t)$.

4 Interference of turbulent and molecular diffusion

In the absence of molecular diffusivity ($\kappa_0 = 0$) the dispersive effect denoted by $D^{\kappa_0=0}(t)$ is referred to as pure turbulent diffusion. In general $\kappa_0 > 0$ and the molecular diffusivity interferes non-trivially with the turbulent diffusivity. Saffman²⁵ has considered this question and by considering solutions of the passive scalar equation on short time and length scales he demonstrates that

$$D(t) = D^{\kappa_0=0}(t) - \frac{1}{9}\kappa_0 t^3 \overline{\omega^2} + O(t^4), \quad (18)$$

for small times t . Here $\overline{\omega^2}$ is the mean-square vorticity. We consider the FDC expansion for the dispersion in a similar form to (17):

$$D(t) = \sum_{n=1}^{\infty} D_n(t),$$

and for small t obtain

$$\begin{aligned} D_1(t) = & D_1^{\kappa_0=0}(t) - \frac{2}{9}\kappa_0 t^3 \int_0^\infty dp p^2 E(p) + \\ & + \frac{1}{18}t^4 \left[\kappa_0^2 \int_0^\infty dp p^4 E(p) - 2\kappa_0 \int_0^\infty dp p^2 E(p) \left. \frac{\partial R}{\partial t} \right|_{t=0} \right] + O(t^5) \end{aligned} \quad (19)$$

$$D_2(t) = D_2^{\kappa_0=0}(t) + O(t^5). \quad (20)$$

Since (see, for example Batchelor²¹)

$$\int_0^\infty dk k^2 E(k) = \frac{1}{2}\overline{\omega^2}$$

and

$$\int_0^\infty dk k^4 E(k) = \frac{1}{2}[\overline{[\nabla \times \omega]^2}],$$

we may rewrite (19) and (20) as

$$D_1(t) = D_1^{\kappa_0=0}(t) - \frac{1}{9}\kappa_0 t^3 \overline{\omega^2} + \frac{1}{18}t^4 \left[\kappa_0^2 \frac{1}{2} \overline{[\nabla \times \omega]^2} - 2\kappa_0 \int_0^\infty dp p^2 E(p) \left. \frac{\partial R}{\partial t} \right|_{t=0} \right] + O(t^5); \quad (21)$$

$$D_2(t) = D_2^{\kappa_0=0}(t) + O(t^5). \quad (22)$$

Evidently to $O(t^3)$ Saffman's conclusion of destructive interference of the molecular diffusivity with the turbulent diffusivity is confirmed by this small-time expansion of the FDC series.

5 The long-term effective diffusivity

We now set the molecular diffusivity κ_0 to zero, in order to examine the mixing effects of the turbulent velocity field. The *long-term effective diffusivity* is defined to be

$$\kappa(\infty) \equiv \lim_{t \rightarrow \infty} \kappa(t)$$

when the limit exists. As a first example, consider a velocity field with energy spectrum

$$E(k) = \frac{3}{2}u^2 \delta(k - k_0) \quad (23)$$

and time correlation function

$$R(t, k) = e^{-|t|/\tau_*}.$$

We nondimensionalize using a reference length k_0^{-1} and a reference time $u^{-1}k_0^{-1}$ (henceforth we use τ_* to represent the nondimensional correlation time), and implement the diagram rules in *Mathematica*. The delta-function spectrum reduces all wavevector integrals to angular integrals, while the time integrals may be done separately and straightforwardly to yield the appropriate power of τ_* . Finally the angular integrals are also performed on *Mathematica*. All integration is done analytically so the results for each diagram

are exact. The following is the expression for the nondimensional long-term diffusivity, correct to order τ_*^9 (i.e. retaining terms up to, and including, $\kappa_5(t)$ in (17)):

$$\kappa(\infty) = \tau_* \left[1 - \frac{1}{2}\tau_*^2 + \frac{11}{24}\tau_*^4 - \frac{4061}{7200}\tau_*^6 + \frac{8775029}{10080000}\tau_*^8 + \dots \right], \quad (24)$$

Note the alternating signs of the coefficients, and the fact that all coefficients are $O(1)$. This series does not converge quickly (if at all), nor should we expect it to—the FDC method is justified as a perturbation method for small correlation time,¹⁹ so we must accept (24) as a possibly divergent asymptotic series.

5.1 Padé approximation

We are thus motivated to examine methods for summing perturbation series. One well-known method is Padé approximation.²⁶ Briefly, given a power series $f(z) = \sum_{n=0}^{\infty} a_n z^n$, the Padé approximant $P_M^N(z)$ is a rational function, i.e., a ratio of two polynomials, with numerator of degree N and denominator of degree M , whose Taylor series agrees with $f(z)$ for the first $N + M + 1$ terms. To examine the Padé approximants to (24) we let $z = \tau_*^2$, and consider the Padé approximants for the term in square brackets in (24):

$$\begin{aligned} P_1^0(z) &= \frac{1}{1 + \frac{1}{2}z} \\ P_1^1(z) &= \frac{1 + \frac{5}{12}z}{1 + \frac{11}{12}z} \\ P_2^1(z) &= \frac{1 + \frac{1661}{1500}z}{1 + \frac{2411}{1500}z + \frac{259}{750}z^2} \\ P_2^2(z) &= \frac{1 + \frac{8514637}{4351200}z + \frac{18482041}{52214400}z^2}{1 + \frac{10690237}{4351200}z + \frac{58691863}{52214400}z^2}. \end{aligned} \quad (25)$$

From Fig. 2 we can see that the Padé approximants appear to be converging and doing so much more rapidly than the basic series (24).

The convergence theory of Padé approximants is chiefly based upon Stieltjes series, i.e., series of the

form

$$\sum_{n=0}^{\infty} a_n (-z)^n,$$

where the coefficients a_n are the moments of a real nonnegative function $\rho(s)$:

$$a_n = \int_0^{\infty} s^n \rho(s) ds, \quad \rho(s) \geq 0 \quad (0 \leq s < \infty).$$

For these series it can be shown^{26,27} that when z is fixed, $P_N^N(z)$ decreases monotonically, $P_{N+1}^N(z)$ increases monotonically, and $P_N^N(z) \rightarrow P_{N+1}^N(z)$ as N increases. Although we cannot prove that our series (24) is a Stieltjes series, the available Padé approximants do indeed have these properties. Thus we conjecture that $\tau_* P_2^1(\tau_*^2)$ provides a lower bound for the nondimensional effective diffusivity and that $\tau_* P_2^2(\tau_*^2)$ provides an upper bound, i.e.,

$$\tau_* P_2^1(\tau_*^2) \leq \kappa(\infty) \leq \tau_* P_2^2(\tau_*^2). \quad (26)$$

Since $P_2^1(\tau_*^2)$ and $P_2^2(\tau_*^2)$ differ by only about 1% even at $\tau_* = 1$, we conclude that (26) gives an accurate approximation for the long term effective diffusivity for (dimensional) correlation times as large as $(uk_0)^{-1}$.

5.2 More general spectra

Even when the energy spectrum does not have the simple delta-function form considered in (23) above, the FDC integrals can always be reduced to multiple integrals over wavenumbers and time by doing all the angular integrals exactly (see appendix). Moreover, for simple forms of the time correlation R , the time integrals may also be done exactly, leaving just wavenumber integrals over the energy spectrum $E(k)$. Using the *Mathematica* program based on the diagram expansion, we have calculated the first few terms in the FDC series for the long-term effective diffusivity for a variety of spectral shapes and time correlation functions. Specifically, we list in Tables I and II results of the form (24) for the following energy spectra

and time correlation functions:

$$\begin{aligned}
E_a(k) &= \frac{3}{2}u^2\delta(k - k_0) \\
E_b(k) &= \frac{4u^2k^4}{\pi^{\frac{1}{2}}k_0^5}\exp(-k^2/k_0^2) \\
E_c(k) &= \begin{cases} \frac{1}{1-(1+\beta)^{-\frac{2}{3}}}u^2k_0^{\frac{2}{3}}k^{-\frac{5}{3}} & \text{for } k_0 < k < (1 + \beta)k_0, \\ 0 & \text{otherwise} \end{cases} \\
R_a(t, k) &= \exp(-\omega_k|t|) \\
R_b(t, k) &= \exp(-\omega_k^2t^2) \\
R_c(t, k) &= \exp(-\omega_k|t|)\cos(2\omega_k t)
\end{aligned}$$

where the ‘‘inverse correlation time’’ ω_k equals one of $1/\tau_*$, k/τ_* or k^2/τ_* . Spectrum E_b is often used to approximate the final stages of decaying turbulence and spectrum E_c models an inertial range. Each spectrum is normalized so that

$$\int_0^\infty E(k)dk = \frac{3}{2}u^2.$$

The time correlation function R_a makes the time integrals very simple; however, it is not differentiable at $t = 0$ and so we include R_b as a more realistic model. Note that both the above time correlation functions are positive for all t ; we also consider the effect of negative loops in the time correlation function when we use R_c .

Padé approximants like (25) for certain cases from Table I are plotted in Figs. 2 to 7. For each case we calculate the integral length

$$l = \frac{3\pi \int_0^\infty k^{-1}E(k)dk}{4 \int_0^\infty E(k)dk}$$

and plot the available approximants for values of the dimensionless correlation time τ_* running from zero up to the (dimensionless) eddy circulation time lk_0 . In general there is not much difference between the

approximations resulting from correlations R_a and R_b (see Figs. 3 and 4), indicating that the shape of the correlation function near $t = 0$ is not critical to the value of $\kappa(\infty)$. Note also that the convergence of the approximations is improved when passing from $\omega_k = 1/\tau_*$ to $\omega_k = k/\tau_*$ to $\omega_k = k^2/\tau_*$ (compare Figs. 5 and 6). In all cases with time correlation R_a and R_b we find behavior of the Padé approximants which we term *Stieltjes-like*, i.e., the power series coefficients alternate in sign, P_N^N decreases monotonically and P_{N+1}^N increases monotonically as N increases, with no poles of the approximants being on the positive real axis. This leads us to conjecture that Padé approximants provide successively improving upper and lower bounds on the long-term effective diffusivity (as they are known to do for Stieltjes series), when the time correlation function is always positive. However, for time correlation R_c the sign pattern of the power series coefficients violates the Stieltjes rule, and indeed we find a pole of the P_1^0 approximant for energy spectrum E_a at $\tau_* = 1.96$. Nevertheless the higher order Padé approximants still converge rapidly (see Fig. 7), so we can still find close approximations for the value of the long-term effective diffusivity, although without the neat bounding behavior of the Stieltjes-like series. The accuracy of these approximations is demonstrated by comparison with numerical calculations of the effective diffusivity in section 8.

6 Generalized Padé approximation for $\kappa(t)$

We wish to generalize the ideas of the preceding section to the calculation of $\kappa(t)$, the effective diffusivity at finite time. Each diagram contribution can be calculated as before and now generates a function of t . We alter the time variable to $\tilde{t} = t/\tau_*$ and change each integration variable to $\tilde{t}_i = t_i/\tau_*$ to pull a factor of τ_*^{2n-1} outside each FDC n integral. The generalization of (24) then has the form

$$\kappa(t) = \tau_* \kappa_1(t/\tau_*) + \tau_*^3 \kappa_2(t/\tau_*) + \tau_*^5 \kappa_3(t/\tau_*) + \dots \quad (27)$$

with $\kappa_n(\infty)$ being the FDC n contribution to the long-term effective diffusivity as calculated previously. For example, for the energy spectrum $E_a(k)$ we know from (24) that $\kappa_1(\infty) = 1$, $\kappa_2(\infty) = -\frac{1}{2}$ and $\kappa_3(\infty) = \frac{11}{24}$. Now we generate the *generalized Padé approximants* to (27) by treating each $\kappa_i(t/\tau_*)$ as if it were a constant coefficient in a τ_* power series. Thus we approximate $\kappa(t)/\tau_*$ by

$$\begin{aligned} P_1^0(\tau_*^2; t) &= \frac{\kappa_1(t/\tau_*)}{1 - \frac{\kappa_2(t/\tau_*)}{\kappa_1(t/\tau_*)} \tau_*^2}, \\ P_1^1(\tau_*^2; t) &= \frac{\kappa_1(t/\tau_*) - \frac{\kappa_1(t/\tau_*)\kappa_3(t/\tau_*) - \kappa_2^2(t/\tau_*)}{\kappa_2(t/\tau_*)} \tau_*^2}{1 - \frac{\kappa_3(t/\tau_*)}{\kappa_2(t/\tau_*)} \tau_*^2}, \end{aligned} \quad (28)$$

and so on. The quadrature expressions for $\kappa_1(\tilde{t})$, $\kappa_2(\tilde{t})$ and $\kappa_3(\tilde{t})$ are listed in the appendix.

In Fig. 8 we fix $\tau_* = 1$ and plot the approximations $\tau_* P_1^0(\tau_*^2; t)$ and $\tau_* P_1^1(\tau_*^2; t)$ to $\kappa(t)$ as functions of the time t . The generalized Padé approximants are found to give good approximations for all t and for τ_* up to order one, i.e., for dimensional correlation times on the order of the eddy circulation time.

7 The Lagrangian correlation

Having introduced the generalized Padé approximation to $\kappa(t)$ for τ_* of order one, we go a step further and consider how this method can approximate the Lagrangian correlation for isotropic turbulence

$$L(t) = \frac{1}{3} \langle u_\alpha(\mathbf{x}_0, 0) u_\alpha(\mathbf{r}(t), t) \rangle,$$

where $\mathbf{r}(t)$ is the position vector of the fluid particle which was at \mathbf{x}_0 at time 0, i.e.,

$$\begin{aligned} \frac{d}{dt} \mathbf{r}(t) &= \mathbf{u}(\mathbf{r}(t), t) \\ \mathbf{r}(0) &= \mathbf{x}_0. \end{aligned} \quad (29)$$

The Lagrangian correlation is a very useful quantity in studies of turbulent diffusion and particle dispersion,¹ but for experimental flows the Eulerian correlation (which is measured at two points fixed

in space, instead of following a fluid particle as for $L(t)$) is much easier to measure. It is therefore of considerable interest to investigate whether a connection can be made between the Lagrangian correlation and the known Eulerian correlation.

It follows from the definition of the Lagrangian correlation that

$$L(t) = \frac{d}{dt}\kappa(t) = \frac{1}{2} \frac{d^2}{dt^2} D(t). \quad (30)$$

As we have already detailed an accurate approximation scheme for $\kappa(t)$, it is straightforward to apply it to $L(t)$. We take the series of FDC n integrals (27) for $\kappa(t)$:

$$\kappa(t) = \tau_* \kappa_1(t/\tau_*) + \tau_*^3 \kappa_2(t/\tau_*) + \dots$$

and differentiate with respect to t to get a series for $L(t)$:

$$L(t) = \frac{d}{dt}\kappa(t) = \kappa'_1(t/\tau_*) + \tau_*^2 \kappa'_2(t/\tau_*) + \dots \quad (31)$$

As each of the $\kappa_i(\tilde{t})$ functions is produced from repeated time integrals, the derivative $\kappa'_i(\tilde{t})$ reduces to an integral of one dimension less than $\kappa_i(\tilde{t})$. For example, the FDC2 term $\kappa_2(\tilde{t})$ is defined by (see appendix):

$$\kappa_2(\tilde{t}) = - \int_0^\infty dk_1 \int_0^\infty dk_2 \int_0^{\tilde{t}} d\tilde{t}_1 \int_0^{\tilde{t}_1} d\tilde{t}_2 \int_0^{\tilde{t}_2} d\tilde{t}_3 E(k_1)E(k_2) \frac{4k_1^2}{9} \tilde{R}(\tilde{t} - \tilde{t}_3, k_1) \tilde{R}(\tilde{t}_1 - \tilde{t}_2, k_2),$$

where $\tilde{R}(\tilde{t}, k) = R(\tau_* \tilde{t}, k)$. This can be put in a more convenient form by employing the change of variables $s_1 = \tilde{t} - \tilde{t}_1, s_2 = \tilde{t}_1 - \tilde{t}_2, s_3 = \tilde{t}_2 - \tilde{t}_3$ to obtain:

$$\kappa_2(\tilde{t}) = - \int_0^\infty dk_1 \int_0^\infty dk_2 \int_0^{\tilde{t}} ds_1 \int_0^{\tilde{t}-s_1} ds_2 \int_0^{\tilde{t}-s_1-s_2} ds_3 E(k_1)E(k_2) \frac{4k_1^2}{9} \tilde{R}(s_1 + s_2 + s_3, k_1) \tilde{R}(s_2, k_2)$$

and then the differentiation is easy to perform:

$$\begin{aligned} \kappa'_2(\tilde{t}) &= - \int_0^\infty dk_1 \int_0^\infty dk_2 \int_0^{\tilde{t}} ds_1 \int_0^{\tilde{t}-s_1} ds_2 E(k_1)E(k_2) \frac{4k_1^2}{9} \tilde{R}(\tilde{t}, k_1) \tilde{R}(s_2, k_2) \\ &= - \int_0^\infty dk_1 \int_0^\infty dk_2 \int_0^{\tilde{t}} d\tilde{t}_1 \int_0^{\tilde{t}_1} d\tilde{t}_2 E(k_1)E(k_2) \frac{4k_1^2}{9} \tilde{R}(\tilde{t}, k_1) \tilde{R}(\tilde{t}_1 - \tilde{t}_2, k_2). \end{aligned}$$

From (31) we generate the generalized Padé approximants for $L(t)$ as we did above for $\kappa(t)$. In the cases we have calculated these converge remarkably quickly, so that $P_1^0(\tau_*^2; t)$ and $P_1^1(\tau_*^2; t)$ give very good approximations even at $\tau_* = 1$. It is therefore worth explicitly recording the approximations these give for $L(t)$ in terms of the Eulerian correlation functions:

$$L(t) = L_1(t/\tau_*) + \tau_*^2 L_2(t/\tau_*) + \dots \quad (32)$$

with

$$L_1(\tilde{t}) = \frac{2}{3} \int_0^\infty dk_1 E(k_1) \tilde{R}(\tilde{t}, k_1)$$

$$L_2(\tilde{t}) = - \int_0^\infty dk_1 \int_0^\infty dk_2 \int_0^{\tilde{t}} d\tilde{t}_1 \int_0^{\tilde{t}_1} d\tilde{t}_2 E(k_1) E(k_2) \frac{4k_1^2}{9} \tilde{R}(\tilde{t}, k_1) \tilde{R}(\tilde{t}_1 - \tilde{t}_2, k_2),$$

and the Padé approximants to $L(t)$ are then

$$P_1^0(\tau_*^2; t) = \frac{L_1(t/\tau_*)}{1 - \frac{L_2(t/\tau_*)}{L_1(t/\tau_*)} \tau_*^2}$$

$$P_1^1(\tau_*^2; t) = \frac{L_1(t/\tau_*) - \frac{L_1(t/\tau_*)L_3(t/\tau_*) - L_2^2(t/\tau_*)}{L_2(t/\tau_*)} \tau_*^2}{1 - \frac{L_3(t/\tau_*)}{L_2(t/\tau_*)} \tau_*^2} \quad (33)$$

In the next section we generate a random velocity field with a given Eulerian spectrum and advect particles according to (29). These numerical simulations show that the FDC-Padé approximations to the Lagrangian correlation are indeed accurate for τ_* of order 1, i.e., for dimensional correlation times on the order of the eddy circulation time (see Fig. 11).

8 Numerical simulation of advection by a random velocity field

We create a random velocity field with prescribed statistics and follow fluid particles as they advect, recording the statistical quantities for comparison with the theory of the previous sections. We consider

Gaussian velocity fields with prescribed energy spectra and time correlation functions. The velocity field is generated using a method based on that used by Kraichnan.²⁸ In each realization, we set

$$\mathbf{u}(\mathbf{x}, t) = A \sum_{n=1}^N \{ \mathbf{z}_n \cos [\mathbf{k}_n \cdot \mathbf{x} + \omega_n t] + \mathbf{y}_n \sin [\mathbf{k}_n \cdot \mathbf{x} + \omega_n t] \}.$$

To ensure incompressibility, we have

$$\mathbf{z}_n = \mathbf{k}_n \times \mathbf{a}_n \text{ and } \mathbf{y}_n = \mathbf{k}_n \times \mathbf{b}_n,$$

with \mathbf{a}_n and \mathbf{b}_n chosen from independent Gaussian distributions. The frequencies ω_n are chosen from a random distribution to produce the desired time correlation function $R(t, k)$. For example, a Gaussian distribution with standard deviation $1/\tau_*$ results in the time correlation function R_b , with inverse correlation time $\omega_k = 1/\tau_*$. The vectors \mathbf{k}_n are chosen from a distribution shaped so as to produce the desired energy spectrum $E(k)$: for $E_a(k)$ the \mathbf{k}_n are isotropically distributed on a sphere of radius k_0 , whereas for $E_b(k)$ each component of \mathbf{k}_n is selected from independent Gaussian distributions of standard deviation k_0 . The amplitude A is chosen so that

$$\begin{aligned} \langle u_\alpha(\mathbf{x}, t) u_\alpha(\mathbf{x}, t) \rangle &= 2 \int_0^\infty E(k) dk \\ &= 3u^2, \end{aligned}$$

so for E_a , $A = (3/2N)^{1/2} uk_0^{-1}$ and for E_b , $A = (1/N)^{1/2} uk_0^{-1}$. The number of modes N is taken to be 100. In Fig. 9 we plot the average over 2000 realizations of $u_\alpha(\mathbf{x}, t) u_\alpha(\mathbf{x} + \mathbf{r}, t)$ as a function of $r = |\mathbf{r}|$ for the spectrum $E_a(k)$ —this is compared to the exact correlation function which is

$$\begin{aligned} \langle u_\alpha(\mathbf{x}, t) u_\alpha(\mathbf{x} + \mathbf{r}, t) \rangle &= 2 \int_0^\infty E_a(k) \frac{\sin(kr)}{kr} dk \\ &= 3u^2 \frac{\sin(k_0 r)}{k_0 r}. \end{aligned}$$

Having obtained a satisfactory velocity field, we proceed to follow fluid particles as they are advected

by:

$$\begin{aligned}\frac{d}{dt}\mathbf{r}(t) &= \mathbf{u}(\mathbf{r}(t), t) \\ \mathbf{r}(0) &= \mathbf{0}.\end{aligned}\tag{34}$$

In each realization, (34) is solved by using a fourth-order predictor-corrector scheme due to Hamming,²⁹ with starting values formed by iteration of Newton’s interpolation formula.³⁰ A time step of 0.2 was found to be satisfactory, and each fluid particle was advected for up to 75 steps (i.e., for a dimensional time $t = 15u^{-1}k_0^{-1}$). The numerical approximations for the effective diffusivity $\kappa(t)$ and the Lagrangian correlation $L(t)$ are then calculated from

$$\begin{aligned}\kappa(t) &= \frac{1}{3N_r} \sum_{i=1}^{N_r} \mathbf{r}^{(i)}(t) \cdot \mathbf{u}^{(i)}(\mathbf{r}^{(i)}(t), t), \\ L(t) &= \frac{1}{3N_r} \sum_{i=1}^{N_r} \mathbf{u}^{(i)}(\mathbf{0}, 0) \cdot \mathbf{u}^{(i)}(\mathbf{r}^{(i)}(t), t).\end{aligned}\tag{35}$$

9 Numerical results

In Figs. 10 and 11 the statistical quantities (35) are compared to the corresponding FDC-Padé approximations which are calculated as described in sections 6 and 7. The number of realizations, N_r , is recorded in the legend. The 95% confidence intervals are marked as error bars. Figure 10 uses energy spectrum E_a and time correlation R_b with $\omega_k = 1/\tau_* = (3/2)^{\frac{1}{2}}$. In Fig. 11 we use the spectrum E_b and time correlation R_b with $\omega_k = k/2^{\frac{1}{2}}$. Thus the space-time correlation function is

$$\frac{E(k)R(t, k)}{4\pi k^2} = \frac{u^2 k^2}{\pi^{\frac{3}{2}} k_0^5} \exp(-k^2/k_0^2) \exp(-\frac{1}{2}u^2 k^2 t^2),$$

which was also used by Saffman.¹⁶ Saffman employs Corrsin’s¹⁷ conjecture to obtain a quasi-normal type closure and further assumes that the mean scalar “cloud” has a Gaussian profile. This results in a nonlinear

differential equation for the dispersion which must be solved numerically. The FDC-Padé approximations are very close to the results of Saffman’s approximation—they are almost indistinguishable in Figs. 10 and 11. We stress again that the FDC-Padé approximations are *explicit* quadrature expressions, in contrast to Saffman’s differential equation which requires numerical solution.

It is clear that the FDC-Padé approximations are extremely good, even for values of the correlation time τ_* of order one. In each case the second approximation P_1^1 gives a small but definite improvement over the first approximation P_1^0 . Even the lowest order Padé approximants give reasonable results which means the lowest order FDC diagrams are all that need to be calculated in order to closely approximate the effective diffusivity and Lagrangian correlation using the methods of sections 6 and 7.

10 Conclusion

We have demonstrated a systematic method for expanding the stochastically nonlinear term which arises in problems of advection by a Gaussian velocity field. Our major results are the approximating equations for the average probability density (12), the effective diffusivity (16), and the Lagrangian correlation (32). The approximations are valid for small velocity correlation time, and are extended to physically relevant times by use of Padé approximants. The extension of these results to non-Gaussian velocity fields is currently under investigation.

11 Acknowledgements

Discussions with Professor P. G. Saffman and Professor D. I. Pullin are gratefully acknowledged. This research was partially supported by the Fulbright Commission and a National University of Ireland Traveling Studentship in Mathematical Physics.

A Appendix

When the molecular diffusivity is zero, the diagram integrals defined in section 3 may be reduced to multiple integrals over wavenumbers and time by doing all the angular integrals exactly. We list here the results for the effective diffusivity up to order three, as defined in equation (16).

$$\kappa_1(\tilde{t}) = \frac{2}{3} \int_0^\infty dk_1 \int_0^{\tilde{t}} d\tilde{t}_1 E(k_1) \tilde{R}(\tilde{t} - \tilde{t}_1, k_1), \quad (36)$$

$$\kappa_2(\tilde{t}) = - \int_0^\infty dk_1 \int_0^\infty dk_2 \int_0^{\tilde{t}} d\tilde{t}_1 \int_0^{\tilde{t}_1} d\tilde{t}_2 \int_0^{\tilde{t}_2} d\tilde{t}_3 E(k_1) E(k_2) \frac{4k_1^2}{9} \tilde{R}(\tilde{t} - \tilde{t}_3, k_1) \tilde{R}(\tilde{t}_1 - \tilde{t}_2, k_2), \quad (37)$$

$$\begin{aligned} \kappa_3(\tilde{t}) = & \int_0^\infty dk_1 \int_0^\infty dk_2 \int_0^\infty dk_3 \int_0^{\tilde{t}} d\tilde{t}_1 \int_0^{\tilde{t}_1} d\tilde{t}_2 \int_0^{\tilde{t}_2} d\tilde{t}_3 \int_0^{\tilde{t}_3} d\tilde{t}_4 \int_0^{\tilde{t}_4} d\tilde{t}_5 E(k_1) E(k_2) E(k_3) \\ & \times \left\{ -\frac{4k_1^2 k_3^2}{135} \tilde{R}(\tilde{t} - \tilde{t}_3, k_1) \tilde{R}(\tilde{t}_1 - \tilde{t}_4, k_2) \tilde{R}(\tilde{t}_2 - \tilde{t}_5, k_3) \right. \\ & - \frac{4k_1^2 k_2^2}{135} \tilde{R}(\tilde{t} - \tilde{t}_3, k_1) \tilde{R}(\tilde{t}_1 - \tilde{t}_5, k_2) \tilde{R}(\tilde{t}_2 - \tilde{t}_4, k_3) \\ & - \frac{4k_1^2 k_3^2}{135} \tilde{R}(\tilde{t} - \tilde{t}_4, k_1) \tilde{R}(\tilde{t}_1 - \tilde{t}_3, k_2) \tilde{R}(\tilde{t}_2 - \tilde{t}_5, k_3) \\ & - \frac{8k_1^2 k_2^2}{135} \tilde{R}(\tilde{t} - \tilde{t}_4, k_1) \tilde{R}(\tilde{t}_1 - \tilde{t}_5, k_2) \tilde{R}(\tilde{t}_2 - \tilde{t}_3, k_3) \\ & + \frac{8k_1^4}{27} \tilde{R}(\tilde{t} - \tilde{t}_5, k_1) \tilde{R}(\tilde{t}_1 - \tilde{t}_2, k_2) \tilde{R}(\tilde{t}_3 - \tilde{t}_4, k_3) \\ & + \frac{8k_1^4}{27} \tilde{R}(\tilde{t} - \tilde{t}_5, k_1) \tilde{R}(\tilde{t}_1 - \tilde{t}_3, k_2) \tilde{R}(\tilde{t}_2 - \tilde{t}_4, k_3) \\ & + \frac{8k_1^4}{27} \tilde{R}(\tilde{t} - \tilde{t}_5, k_1) \tilde{R}(\tilde{t}_1 - \tilde{t}_4, k_2) \tilde{R}(\tilde{t}_2 - \tilde{t}_3, k_3) \\ & \left. + \frac{8k_1^2 k_2^2}{27} \tilde{R}(\tilde{t} - \tilde{t}_5, k_1) \tilde{R}(\tilde{t}_1 - \tilde{t}_4, k_2) \tilde{R}(\tilde{t}_2 - \tilde{t}_3, k_3) \right\}. \quad (38) \end{aligned}$$

Differentiation of these formulas with respect to time (see (31)) gives the approximation (32) for the Lagrangian correlation $L(t)$.

References

- [1] G. T. Csanady, *Turbulent diffusion in the environment*, (D. Reidel Publishing Company, 1973).
- [2] D. S. Dean, I. T. Drummond and R. R. Horgan, “Perturbation schemes for flow in random media,” *J. Phys. A* **27**, 5135 (1994).
- [3] R. Phythian and W. D. Curtis, “The effective long-term diffusivity for a passive scalar in a Gaussian model fluid flow,” *J. Fluid Mech.* **89**, 241 (1978).
- [4] P. H. Roberts, “Analytical theory of turbulent diffusion,” *J. Fluid Mech.* **11**, 257 (1961).
- [5] R. H. Kraichnan, “The structure of isotropic turbulence at very high Reynolds numbers,” *J. Fluid Mech.* **5**, 497 (1959).
- [6] R. H. Kraichnan, “Small-scale structure of a scalar field convected by turbulence,” *Phys. Fluids* **11**, 945 (1968).
- [7] T. Elperin, N. Kleeorin and I. Rogachevskii, “Turbulent thermal diffusion of small inertial particles,” *Phys. Rev. Lett.* **76**, 224 (1996).
- [8] D. Bernard, K. Gawedzki and A. Kupiainen, “Anomalous scaling in the N-point functions of a passive scalar,” *Phys. Rev. E* **54**, 2564 (1996).
- [9] M. Chertkov and G. Falkovich, “Anomalous scaling exponents of a white-advected passive scalar,” *Phys. Rev. Lett.* **76**, 2706 (1996).
- [10] T. Elperin, N. Kleeorin and I. Rogachevskii, “Anomalous scalings for fluctuations of inertial particles concentration and large-scale dynamics,” *Phys. Rev. E* **58**, 3113 (1998).

- [11] N. A. Silant'ev, "Comparison of methods for calculating turbulent diffusion coefficients," Sov. Phys. JETP **84**, 479 (1997).
- [12] G. Comte-Bellot and S. Corrsin, "Space-time correlation measurements in isotropic turbulence," J. Fluid Mech. **48**, 273 (1971).
- [13] T. Sanada and V. Shanmugasundaram, "Random sweeping effect in isotropic numerical turbulence," Phys. Fluids A **4**, 1245 (1992).
- [14] W. D. McComb, V. Shanmugasundaram and P. Hutchinson, "Velocity-derivative skewness and two-time velocity correlations of isotropic turbulence as predicted by the LET theory," J. Fluid Mech. **208**, 91 (1989).
- [15] G. I. Taylor, "Diffusion by continuous movements," Proc. Lond. Math. Soc. A **20**, 196 (1921).
- [16] P. G. Saffman, "An approximate calculation of the Lagrangian auto-correlation coefficient for stationary homogeneous turbulence," Appl. Sci. Res. **A 11**, 245 (1961).
- [17] S. Corrsin, "Progress report on some turbulent diffusion problems," Adv. Geophys. **6**, 161 (1959).
- [18] R. E. Davis, "On relating Eulerian and Lagrangian velocity statistics: single particles in homogeneous flows," J. Fluid Mech. **114**, 1 (1982).
- [19] J. P. Gleeson, *Random advection of a passive scalar*, Ph.D. thesis, (California Institute of Technology, 1999).
- [20] E.A. Novikov, "Functionals and the random-force method in turbulence," Sov. Phys. JETP **20**, 1290 (1965).
- [21] G. K. Batchelor, *The theory of homogeneous turbulence*, p.49 (Cambridge University Press, 1953).

- [22] J. Zinn-Justin, *Quantum field theory and critical phenomena*, 3rd ed. p.5 (Oxford University Press, 1996).
- [23] R. H. Kraichnan, “Dynamics of nonlinear stochastic systems,” *J. Math. Phys.* **2**, 124 (1961).
- [24] S. A. Orszag, “Lectures on the statistical theory of turbulence” in *Fluid Dynamics, Les Houches 1973*, eds. R. Balian and J. L. Peule, (Gordon and Breach, 1973).
- [25] P. G. Saffman, “On the effect of the molecular diffusivity in turbulent diffusion,” *J. Fluid Mech.* **8**, 273 (1960).
- [26] C. M. Bender and S. A. Orszag, *Advanced mathematical methods for scientists and engineers*, (McGraw-Hill, 1978).
- [27] G. A. Baker, *Essentials of Padé approximants*, (Academic Press, 1975).
- [28] R. H. Kraichnan, “Diffusion by a random velocity field,” *Phys. Fluids* **13**, 22 (1970).
- [29] R. W. Hamming, “Stable predictor corrector methods for ordinary differential equations,” *J. Assoc. Comp. Math.* **6**, 37 (1959).
- [30] A. Ralston, “Numerical integration methods for the solution of ordinary differential equations” in *Mathematical methods for digital computers*, eds. A. Ralston and H. S. Wilf, (John Wiley & Sons, 1960).

List of Tables

I	Coefficients of the FDC series for the long-term effective diffusivity.	29
II	Padé approximations to the FDC series in Table I.	30

Energy spectrum	Time correlation	ω_k	Coeff. of τ_*	Coeff. of τ_*^3	Coeff. of τ_*^5	Coeff. of τ_*^7	Figure
E_a	R_a	$1/\tau_*$	1.000	-0.500	0.459	-0.564	2
E_a	R_b	$1/\tau_*$	0.886	-0.184	0.050		
E_a	R_c	$1/\tau_*$	0.200	0.052	-0.016	0.0047	
E_b	R_a	$1/\tau_*$	1.000	-1.250	3.906	-19.13	
E_b	R_a	k/τ_*	0.753	-0.352	0.323	-0.413	3
E_b	R_a	k^2/τ_*	0.667	-0.222	0.140	-0.116	
E_b	R_b	$1/\tau_*$	0.886	-0.459	0.429		
E_b	R_b	k/τ_*	0.667	-0.128	0.034		4
E_b	R_b	k^2/τ_*	0.591	-0.087	0.019		
E_b	R_c	k/τ_*	0.113	0.034	-0.007	0.0013	
$E_c, \beta = 1$	R_a	$1/\tau_*$	1.000	-1.027	2.221	-6.925	
$E_c, \beta = 10$	R_a	$1/\tau_*$	1.000	-7.35	318.1	-23711	
$E_c, \beta = 1$	R_a	k/τ_*	0.741	-0.363	0.333	-0.416	
$E_c, \beta = 10$	R_a	k/τ_*	0.492	-0.211	0.189	-0.254	5
$E_c, \beta = 1$	R_a	k^2/τ_*	0.569	-0.162	0.085	-0.060	6
$E_c, \beta = 10$	R_a	k^2/τ_*	0.313	-0.049	0.015	-0.006	

Table I: Coefficients of the FDC series for the long-term effective diffusivity.

Energy spectrum	Time correlation	ω_k	$P_1^0(\tau_*^2)$ at $\tau_* = 1$	$P_1^1(\tau_*^2)$ at $\tau_* = 1$	$P_2^1(\tau_*^2)$ at $\tau_* = 1$	Figure
E_a	R_a	$1/\tau_*$	0.667	0.739	0.714	2
E_a	R_b	$1/\tau_*$	0.734	0.742		
E_a	R_c	$1/\tau_*$	0.270	0.240	0.240	
E_b	R_a	$1/\tau_*$	0.444	0.697	0.541	
E_b	R_a	k/τ_*	0.513	0.569	0.549	3
E_b	R_a	k^2/τ_*	0.500	0.530	0.522	
E_b	R_b	$1/\tau_*$	0.584	0.649		
E_b	R_b	k/τ_*	0.559	0.565		4
E_b	R_b	k^2/τ_*	0.515	0.520		
E_b	R_c	k/τ_*	0.160	0.140	0.140	
$E_c, \beta = 1$	R_a	$1/\tau_*$	0.493	0.675	0.578	
$E_c, \beta = 10$	R_a	$1/\tau_*$	0.120	0.834	0.208	
$E_c, \beta = 1$	R_a	k/τ_*	0.497	0.551	0.532	
$E_c, \beta = 10$	R_a	k/τ_*	0.345	0.381	0.367	5
$E_c, \beta = 1$	R_a	k^2/τ_*	0.443	0.463	0.458	6
$E_c, \beta = 10$	R_a	k^2/τ_*	0.271	0.275	0.274	

Table II: Padé approximations to the FDC series in Table I.

List of Figures

1	The FDC diagrams of order 1 and 2 (which represent the FDC2 approximation (12)).	32
2	The FDC5 approximation to $\kappa(\infty)$ and its Padé approximants for spectrum E_a , time correlation R_a and $\omega_k = 1/\tau_*$	33
3	Padé approximants for $\kappa(\infty)$ for spectrum E_b , time correlation R_a and $\omega_k = k/\tau_*$	34
4	Padé approximants for $\kappa(\infty)$ for spectrum E_b , time correlation R_b and $\omega_k = k/\tau_*$	35
5	Padé approximants for $\kappa(\infty)$ for spectrum E_c ($\beta = 10$), time correlation R_a and $\omega_k = k/\tau_*$	36
6	Padé approximants for $\kappa(\infty)$ for spectrum E_c ($\beta = 10$), time correlation R_a and $\omega_k = k^2/\tau_*$	37
7	Padé approximants for $\kappa(\infty)$ for spectrum E_a , time correlation R_c and $\omega_k = 1/\tau_*$. P_1^0 has a pole at $\tau_* = 1.96$, but P_1^1 and P_2^1 have no poles on the positive real axis.	38
8	Generalized Padé approximants for $\kappa(t)$ for spectrum E_a , time correlation R_a and $\omega_k = 1/\tau_*$, with $\tau_* = 1$	39
9	Comparison of exact (solid line) and numerical (symbols) correlation functions for spectrum E_a	40
10	Generalized Padé and the Saffman (1961) approximations (lines) and numerical values (dots) for $\kappa(t)$ for spectrum E_a , time correlation R_b and $\omega_k = 1/\tau_*$. Here τ_* is fixed, $\tau_* = (2/3)^{\frac{1}{2}}$	41
11	Generalized Padé and the Saffman (1961) approximations (lines) and numerical values (dots) for $L(t)$ for spectrum E_b , time correlation R_b and $\omega_k = k/\tau_*$. Here τ_* is fixed, $\tau_* = 2^{\frac{1}{2}}$	42

$$\frac{\partial}{\partial t} \hat{\Theta}(\mathbf{k}, t) + \kappa_0 k^2 \hat{\Theta}(\mathbf{k}, t) =$$

Figure 1: The FDC diagrams of order 1 and 2 (which represent the FDC2 approximation (12)).

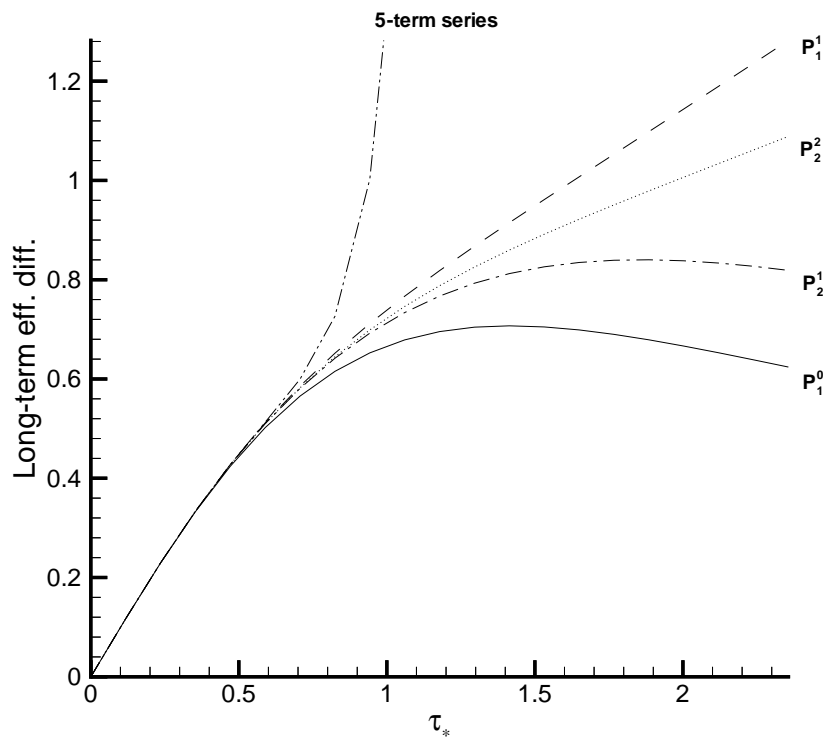


Figure 2: The FDC5 approximation to $\kappa(\infty)$ and its Padé approximants for spectrum E_a , time correlation R_a and $\omega_k = 1/\tau_*$.

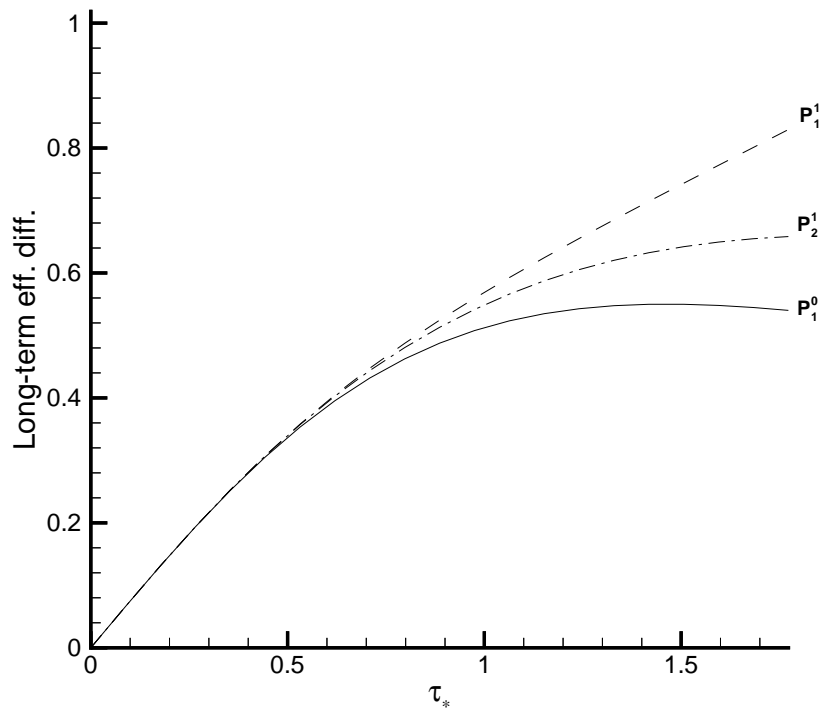


Figure 3: Padé approximants for $\kappa(\infty)$ for spectrum E_b , time correlation R_a and $\omega_k = k/\tau_*$.

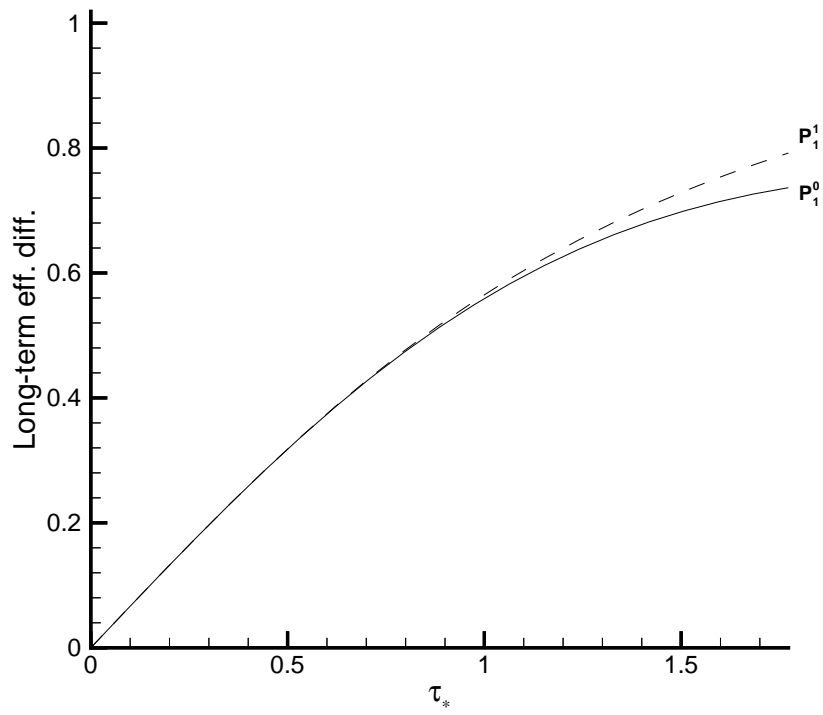


Figure 4: Padé approximants for $\kappa(\infty)$ for spectrum E_b , time correlation R_b and $\omega_k = k/\tau_*$.

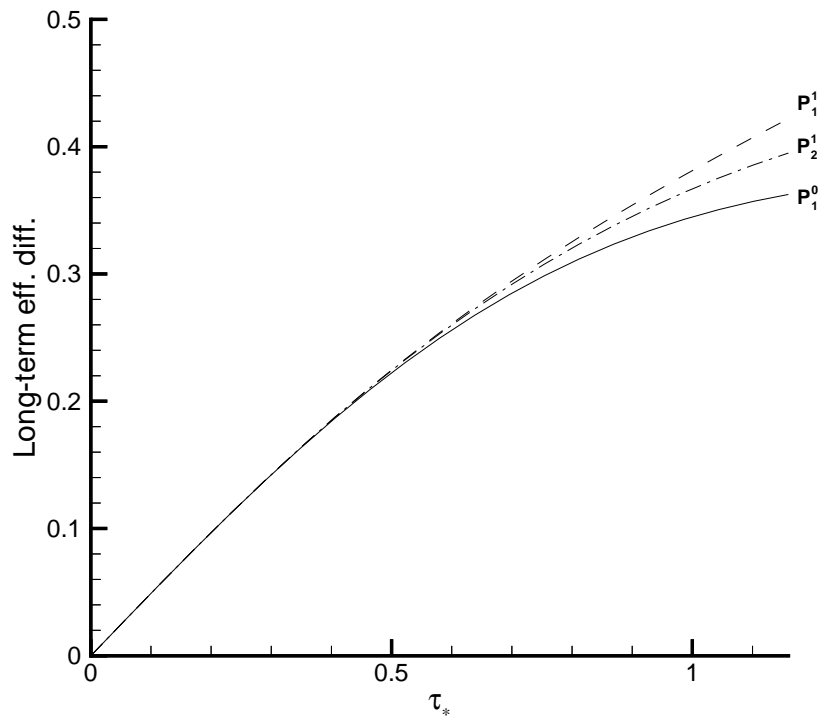


Figure 5: Padé approximants for $\kappa(\infty)$ for spectrum E_c ($\beta = 10$), time correlation R_a and $\omega_k = k/\tau_*$.

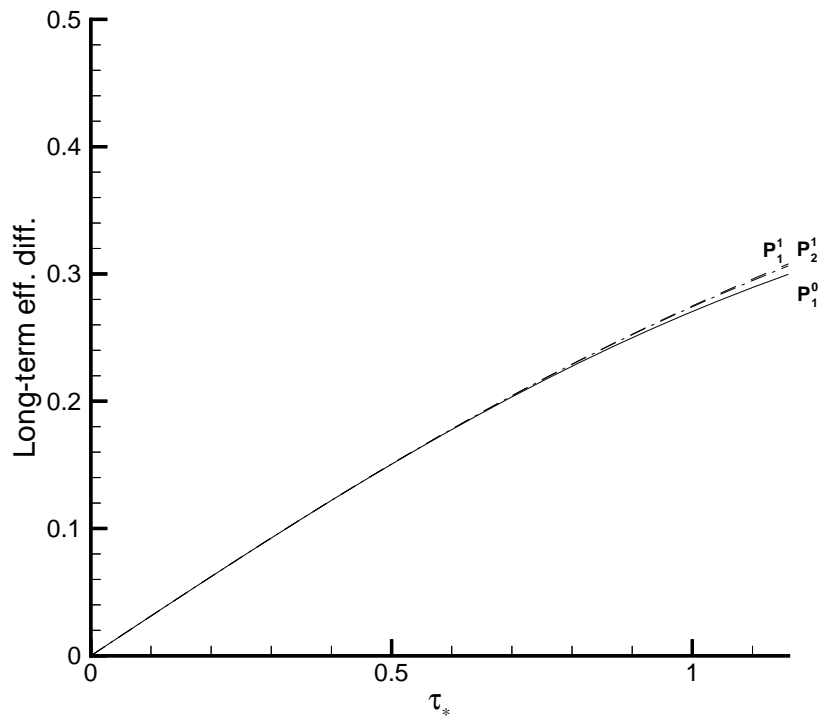


Figure 6: Padé approximants for $\kappa(\infty)$ for spectrum E_c ($\beta = 10$), time correlation R_a and $\omega_k = k^2/\tau_*$.

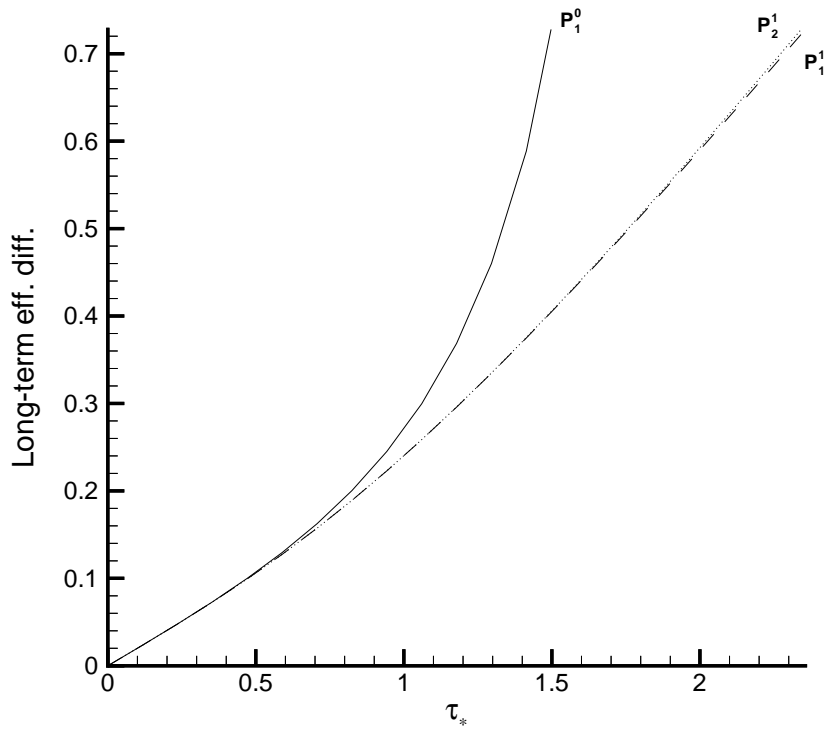


Figure 7: Padé approximants for $\kappa(\infty)$ for spectrum E_a , time correlation R_c and $\omega_k = 1/\tau_*$. P_1^0 has a pole at $\tau_* = 1.96$, but P_1^1 and P_2^1 have no poles on the positive real axis.

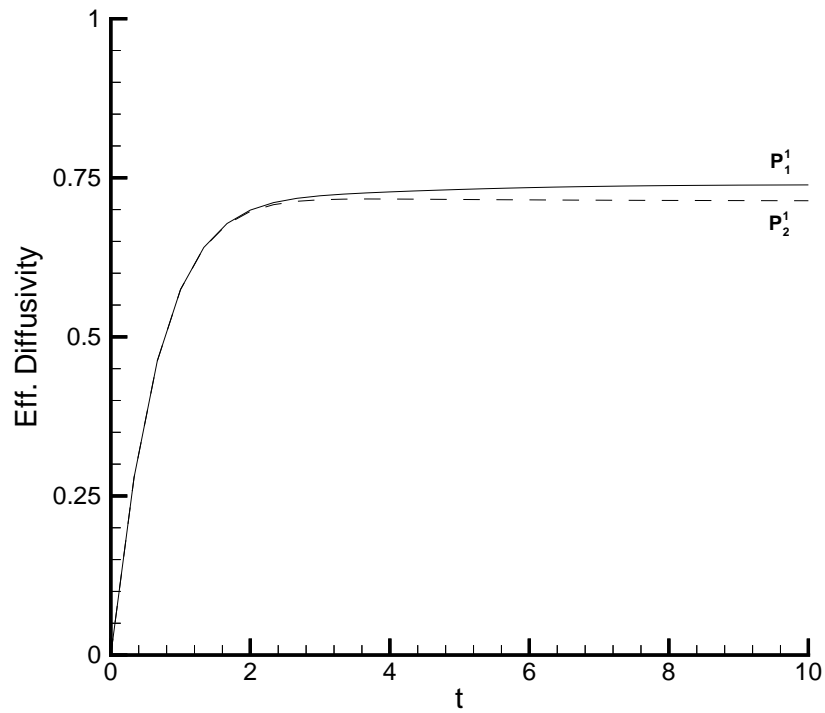


Figure 8: Generalized Padé approximants for $\kappa(t)$ for spectrum E_a , time correlation R_a and $\omega_k = 1/\tau_*$, with $\tau_* = 1$.

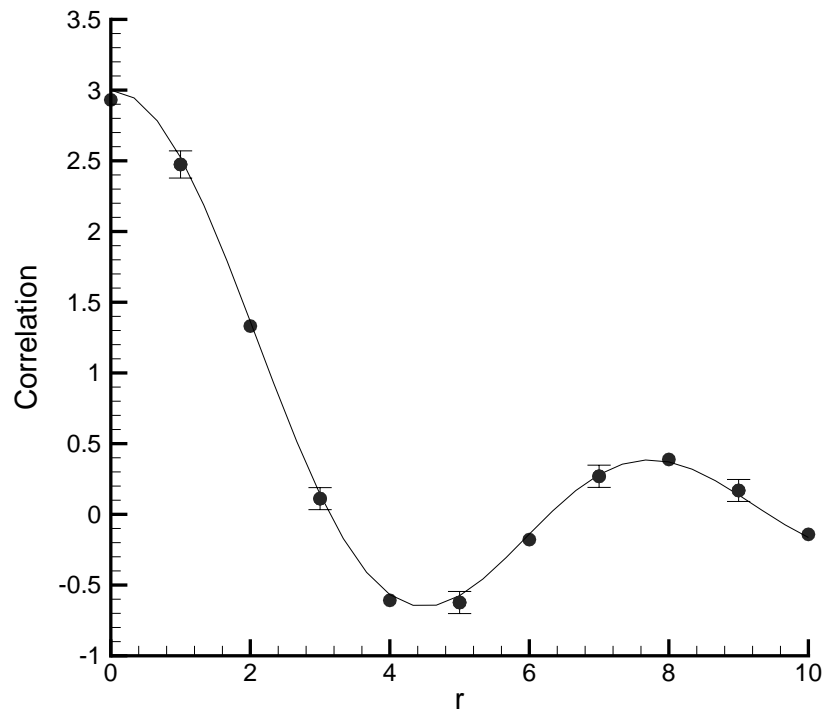


Figure 9: Comparison of exact (solid line) and numerical (symbols) correlation functions for spectrum E_a .

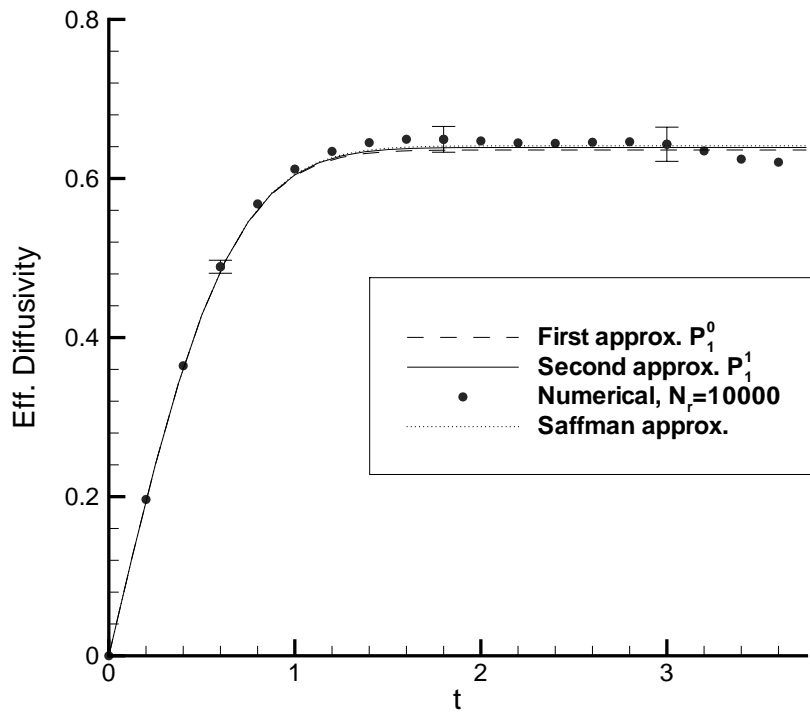


Figure 10: Generalized Padé and the Saffman (1961) approximations (lines) and numerical values (dots) for $\kappa(t)$ for spectrum E_a , time correlation R_b and $\omega_k = 1/\tau_*$. Here τ_* is fixed, $\tau_* = (2/3)^{\frac{1}{2}}$.

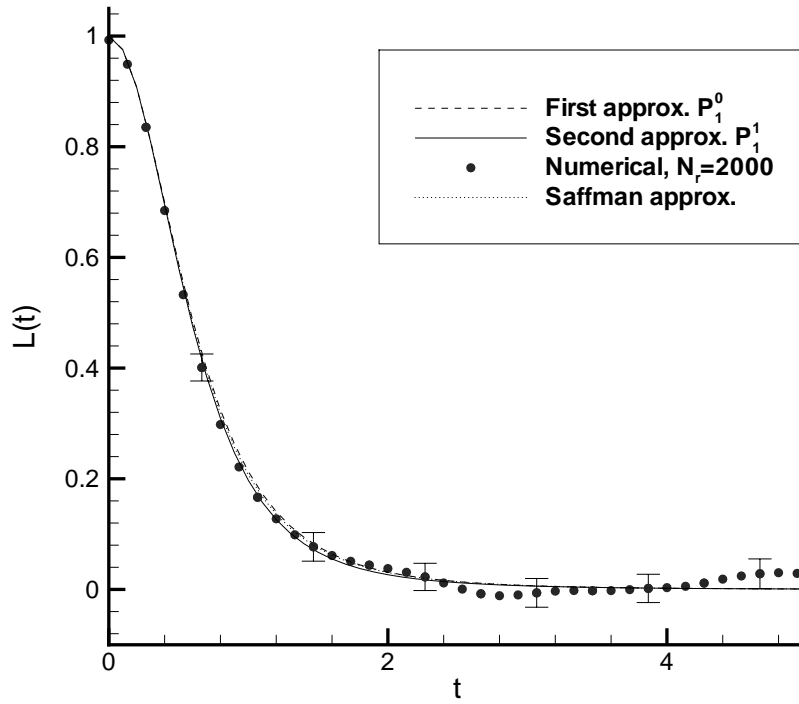


Figure 11: Generalized Padé and the Saffman (1961) approximations (lines) and numerical values (dots) for $L(t)$ for spectrum E_b , time correlation R_b and $\omega_k = k/\tau_*$. Here τ_* is fixed, $\tau_* = 2^{\frac{1}{2}}$.